

SUPERWASP J015100.23-100524.2: A SPOTTED SHALLOW-CONTACT BINARY BELOW THE PERIOD LIMIT

S. B. QIAN^{1,2,3}, B. ZHANG^{1,2,3}, B. SOONTHORNTHUM⁴, J. J. HE^{1,2}, S. RATTANASOON⁴, S. AUKKARAVITTAYAPUN⁴, L. LIU^{1,2,3},
L. Y. ZHU^{1,2,3}, E. G. ZHAO^{1,2,3}, X. ZHOU^{1,2,3}, AND S. THAWICHARAT^{1,3,4}

¹ Yunnan Observatories, Chinese Academy of Sciences (CAS), P.O. Box 110, 650011 Kunming, P.R. China; qsb@ynao.ac.cn

² Key laboratory of the structure and evolution celestial bodies, Chinese Academy of Sciences, P.O. Box 110, 650011 Kunming, P. R. China

³ University of the Chinese Academy of Sciences, Yuquan Road 19#, Sijingshang Block, 100049 Beijing, P. R. China

⁴ National Astronomical Research Institute of Thailand, 191 Siriphanich Bldg., Huay Kaew Road, Chiang Mai 50200, Thailand

Received 2015 May 19; accepted 2015 August 11; published 2015 September 18

ABSTRACT

SuperWASP J015100.23-100524.2 (hereafter J015100) is an eclipsing binary with an orbital period of $0^d.2145$ that is below the short-period limit of contact binary stars. Complete light curves of J015100 in B, V, R, and I bands are presented and are analyzed with the Wilson–Devinney method. It has been discovered that J015100 is a shallow-contact binary ($f = 14.6(\pm 2.7)\%$) with a mass ratio of 3.128. It is a W-type contact binary where the less massive component is about 130 K hotter than the more massive one. The asymmetries of light curves are explained as one dark spot on the more massive component. The detection of J015100 as a contact binary below the period limit suggests that contact binaries below this limit are not rapidly destroyed. This shallow-contact system may be formed from a detached short-period binary similar to DV Psc (Sp. = K4/K5; $P = 0^d.30855$) via orbital shrinkage due to angular momentum loss through magnetic stellar wind.

Key words: binaries: close – binaries: eclipsing – stars: evolution – stars: individual (J015100)

1. INTRODUCTION

W UMa-type variable stars are contact binary systems where both cool components are in contact with each other and share a common convective envelope. Although low-mass cool dwarfs are very common, the way they evolve into contact binaries is poorly understood. It is well known that contact binary systems exhibit a fairly sharp lower limit of around 0.22 days to their orbital periods (e.g., Rucinski & Pribulla 2008). Contact binaries under the short-period limit are very rare (e.g., Rucinski 1992; Becker et al. 2011), and only a few contact systems below this period limit were detected, e.g., GSC 0137-00475 with an orbital period of 0.2178 (Rucinski & Pribulla 2008), the red-dwarf contact binary SDSS J001641-000925 with an orbital period of 0.1985615 days (Davenport et al. 2013; Qian et al. 2015).

Explanations for this cutoff included that the component stars are reaching the full convective limit (Rucinski 1992) or that they are difficult to produce because the angular momentum loss (AML) timescale is much longer (e.g., Stepień 2006, 2011), or are so unstable that they are rapidly destroyed (e.g., Qian et al. 2015). However, the convective limit would not provide a full explanation (Rucinski 1992), and Stepień’s low-mass limit does not appear to hold true for some recently discovered systems (e.g., Lohr et al. 2012). By monitoring the red-dwarf contact binary SDSS J001641-000925 for several years, Qian et al. (2015) found that the rapid decrease in the orbital period of SDSS J001641-000925 is not true, indicating that red-dwarf contact binaries may be stable and are not rapidly destroyed. The rarity of contact binaries under the limit is still an open question and may be the result of a combination of factors, e.g., the component stars reach the full convective limit, are difficult to produce, and are still very difficult to detect, etc.

Thanks to several surveys in the world (e.g., SDSS, the Wide-field Camera (WFCAM) Transit Survey, and SuperWASP), some short-period ($P < 0.22$ days) close binaries were discovered under the limit. Becker et al. (2011) discovered

28 M-dwarf binary systems whose light-curve shapes suggest they are contact binaries in the “Stripe82” region of the Sloan Digital Sky Survey. Norton et al. (2011) presented evidence for 53 candidate W UMa-type eclipsing binaries with periods close to the short-period limit by using SuperWASP data. Later, 143 more candidate objects were reported by Lohr et al. (2012). By using the data from the WFCAM Transit Survey, Nefs et al. (2012) discovered four ultra-short-period ($P < 0.18$ days) eclipsing M-dwarf binaries whose orbital periods are significantly below the sharp period cutoff at $P \sim 0.22$ days. Observations and investigations of close binaries below the period limit can provide valuable information on the origin and evolution of contact binaries (e.g., Qian et al. 2014a). SuperWASP J015100.23-100524.2 (hereafter J015100) is a W UMa-type binary discovered by Lohr et al. (2012) with an orbital period of $0^d.2145$. The light variability in the V band is from 14.73 to 15.15 mag. In this paper, complete multi-color CCD light curves in the B, V, R, and I bands are presented and are analyzed with the Wilson–Devinney (W–D) program (Wilson & Devinney 1971). Then, based on those photometric results, the activity, the structure, and the evolutionary state of the short-period solar-type binary are discussed.

2. COMPLETE CCD PHOTOMETRIC MULTI-COLOR LIGHT CURVES

The 2.4 m Thai National Telescope (TNT) of the National Astronomical Research Institute of Thailand is located on one of the highest ridges of Doi Inthanon (about 2457 m above sea level), the tallest peak in Thailand. The site has good observing conditions in terms of seeing and photometric conditions during the dry season that runs approximately from November to April. The TNT was erected in 2012 and inaugurated in 2013 January. It is a Ritchey–Chrétien with two Nasmyth focuses. A research-grade $4K \times 4K$ CCD photometer with a BVRI filter system was equipped on one of the Nasmyth focuses. The camera is a cryogenically cooled (liquid nitrogen, -110°C) dewar holding a E2V232-84 thinned, astronomy broadband

Table 1
Coordinates of J015100, the Comparison Star, and the Check Star

Targets	α_{2000}	δ_{2000}	B	R
J015100	01 ^h 51 ^m 00 ^s .2	-10°05'24".2	15.3	14.7
The comparison	01 ^h 51 ^m 11 ^s .2	-10°07'20".6	15.5	14.7
The check	01 ^h 50 ^m 56 ^s .1	-10°04'32".9	16.0	15.3

AR-coated, grade-one CCD. It contains $4096 \times 4096 \times 15.0 \mu\text{m}$ pixels with an imaging area of 61.44 mm squared. The field of view is about 8.8×8.8 at the focus.

J015100 was observed on 2014 November 23 with the TNT. During the observations, the standard Johnson–Bessel BVRI filters were used. The integration times were 20 s for the I, R, V, and B filters. PHOT (measure magnitudes for a list of stars) of the aperture photometry package of IRAF⁵ was used to reduce the observed images. One star that is very close to J015100 was chosen as the comparison star. The coordinates of J015100, the comparison star, and the check star are listed in Table 1. A finding chart of J015100 is shown in Figure 1. Also shown in the figure as “C” and “Ch” are the comparison and the check stars, respectively. Complete light curves in the B, V, R, and I bands were obtained on 2014 November 23, and those photometric data are listed in Tables 2–5. The corresponding light curves are shown in Figure 2, and also shown in the figure are the magnitude differences between the comparison and the check stars. The figure displays that the comparison star is not variable during the observation. Based on those data, several times of light minimum were determined and are shown in Table 6, where “Pri” refers to the primary minima, while “Sec” refers to the secondary ones. Since the light curves are symmetric, those eclipse times were determined by fitting a parabola to the deepest part of the eclipse.

As shown in Figure 2, the light curves in four colors are the typical EW-type where light variations are continuous and have a very small difference between the depths of the two minima. These properties reveal tidally distorted components and both of the components have a similar temperature. The amplitudes of the light variation are ~ 0.668 mag in the B band, ~ 0.621 mag in the V band, ~ 0.604 mag in the R band, and ~ 0.573 mag in the I band, respectively. The light curves are asymmetric and show a negative O’Connell effect where the maxima following the primary minima are higher than the other maxima. The differences between the two light maxima are about 0.08 mag in B, 0.06 mag in V, 0.05 mag in V, and 0.03 mag in I, respectively.

3. PHOTOMETRIC SOLUTIONS WITH THE W-D METHOD

To determine photometric elements and to understand the geometrical structure and evolutionary state of the binary star, those multi-color light curves in the BVRI bands were analyzed with the W-D program (Wilson & Devinney 1971; Wilson 1990). The phases of those data were computed with the following linear ephemeris:

$$\text{Min. } I(\text{HJD}) = 2456085.18466 + 0^{\text{d}}.2145001 \times E. \quad (1)$$

⁵ IRAF (an acronym for Image Reduction and Analysis Facility) is a collection of software written at the National Optical Astronomy Observatory (NOAO) geared toward the reduction of astronomical images in pixel array form.

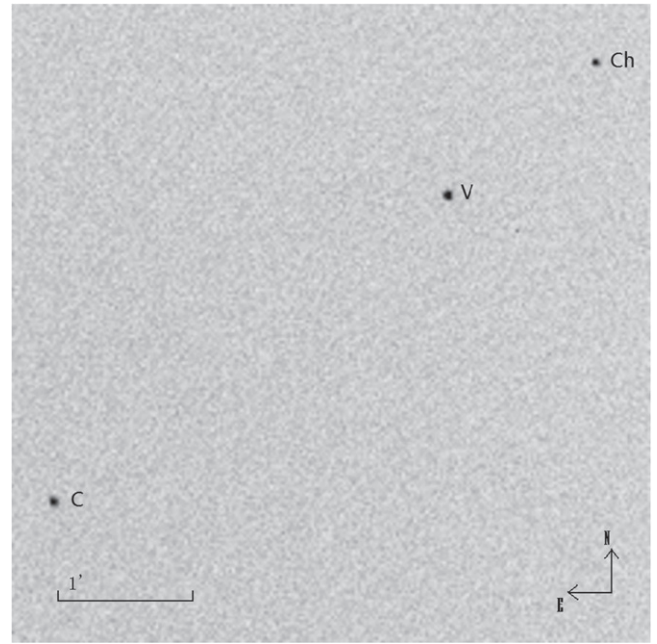


Figure 1. Finding chart of the variable star (J015100). Also shown as “C” and “Ch” are the comparison and the check stars, respectively.

Table 2
CCD Photometric Data of J015100 in the B Band Obtained with the 2.4 m Thai National Telescope (TNT) on 2014 November 23

JD(Hel.)	Phase	Δm
2400000+		
56085.01210	0.1955	-0.492
56085.01267	0.1982	-0.499
56085.01355	0.2023	-0.513
56085.01896	0.2275	-0.508
56085.02097	0.2369	-0.503

Note. The phases are computed by using the ephemeris in Equation (1).

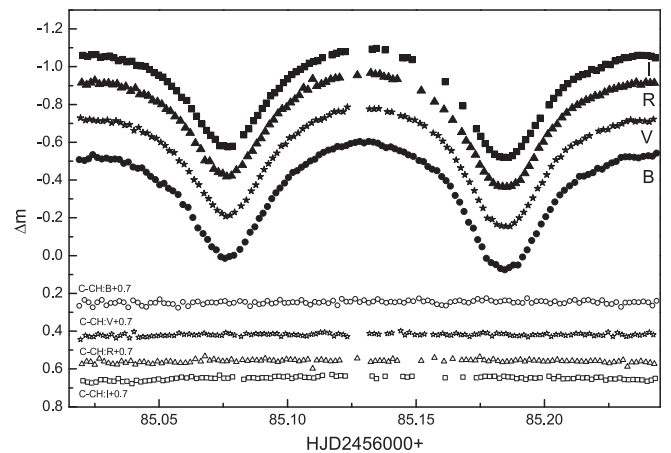


Figure 2. CCD photometric light curves of J015100 observed on 2014 November 23 by using the TNT. Solid circles, stars, triangles, and squares refer to the B, V, R, and I bands, respectively. Magnitude differences between the comparison and the check stars are also shown as open ones.

The initial epoch in the equation is a mean epoch of the new times of primary light minima (see Table 6). According to the 2MASS survey, the colors of the binary star are: $J-H = 0.540$,

Table 3

CCD Photometric Data of J015100 in the V Band Obtained with the 2.4 m Thai National Telescope (TNT) on 2014 November 23

JD(Hel.) 2400000+	Phase	Δm
56085.01950	0.2300	-0.728
56085.02140	0.2389	-0.716
56085.02302	0.2464	-0.722
56085.02460	0.2538	-0.716
56085.02633	0.2619	-0.714

Note. The phases are computed by using the ephemeris in Equation (1).

Table 4

CCD Photometric Data of J015100 in the R Band Obtained with the 2.4 m Thai National Telescope (TNT) on 2014 November 23

JD(Hel.) 2400000+	Phase	Δm
56085.01995	0.2321	-0.916
56085.02183	0.2409	-0.904
56085.02342	0.2483	-0.916
56085.02500	0.2557	-0.927
56085.02680	0.2640	-0.908

Note. The phases are computed by using the ephemeris in Equation (1).

Table 5

CCD Photometric Data of J015100 in the I Band Obtained with the 2.4 m Thai National Telescope (TNT) on 2014 November 23

JD(Hel.) 2400000+	Phase	Δm
56085.02041	0.2343	-1.060
56085.02225	0.2428	-1.054
56085.02381	0.2501	-1.063
56085.02550	0.2580	-1.065
56085.02728	0.2663	-1.051

Note. The phases are computed by using the ephemeris in Equation (1).

Table 6

New CCD Times of the Light Minimum

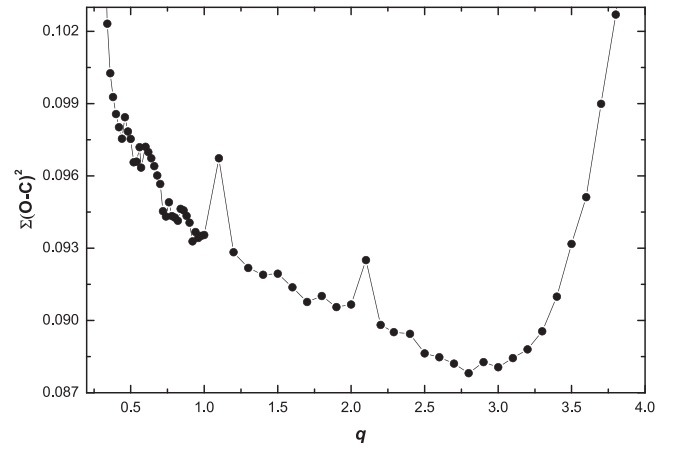
HJD (days)	Errors (days)	Filters	Type
2456085.07648	0.00010	B	Sec
2456085.07656	0.00009	V	Sec
2456085.07628	0.00015	R	Sec
2456085.07651	0.00011	I	Sec
2456085.18481	0.00014	B	Pri
2456085.18477	0.00012	V	Pri
2456085.18469	0.00004	R	Pri
2456085.18436	0.00003	I	Pri

H-K = 0.112, and V-K = 2.804, which correspond to a spectral type of K2–K5. The situations of J015100 are the same as those of CC Com. Its spectral type is K4/5 V with an orbital period of 0.2207 days (e.g., Pribulla et al. 2007). During their photometric solution, Maceroni et al. (1982) chose a temperature of $T_1 = 4500$ for the primary star of CC Com. Therefore, the temperature for star 1 (star eclipsed at primary light minimum) in J015100 was fixed as ($T_1 = 4500$) for our solution.

Table 7

Fixed Parameters during Photometric Solution

Parameters	Values
$g_1 = g_2$	0.32
$A_1 = A_2$	0.5
$x_{1\text{bol}}, x_{2\text{bol}}$	0.313, 0.281
$y_{1\text{bol}}, y_{2\text{bol}}$	0.366, 0.394
$x_{1\text{B}}, x_{2\text{B}}$	1.176, 1.184
$y_{1\text{B}}, y_{2\text{B}}$	-0.388, -0.454
$x_{1\text{V}}, x_{2\text{V}}$	0.785, 0.785
$y_{1\text{V}}, y_{2\text{V}}$	0.016, 0.015
$x_{1\text{R}}, x_{2\text{R}}$	0.492, 0.491
$y_{1\text{R}}, y_{2\text{R}}$	0.276, 0.424
$x_{1\text{I}}, x_{2\text{I}}$	0.300, 0.288
$y_{1\text{I}}, y_{2\text{I}}$	0.387, 0.607
T_1	4500 K

**Figure 3.** The relation between Σ and q .

Gravity darkening coefficients and the bolometric albedo are obtained from Lucy (1967) as $g_1 = g_2 = 0.32$ and from Rucinski (1969) as $A_1 = A_2 = 0.5$ because both components are cool dwarf stars. The bolometric limb-darkening coefficients $x_{1\text{bolo}}$ and $x_{2\text{bolo}}$ and the passband-specific limb-darkening coefficients were chosen from van Hamme (1993) and are listed in Table 7. For a detailed treat of limb darkening, we used the square-root functions for both the bolometric and bandpass limb-darkening laws. First, we assumed that the bolometric and passband-specific limb-darkening coefficients for both components are equal. After determining the temperature of the secondary star, the values for the secondary were redetermined according to its real temperature. We found that solutions converged at mode 3 during the solution. The adjustable parameters are: the orbital inclination i ; the mean temperature of star 2, T_2 ; the monochromatic luminosity of star 1, $L_{1\text{B}}, L_{1\text{V}}, L_{1\text{R}},$ and $L_{1\text{I}}$; and the dimensionless potential ($\Omega_1 = \Omega_2$ for mode 3).

Since no reliable mass ratios were obtained before, we determine the mass ratio by using a q -search method. We search for solutions with mass ratios from 0.25 to 5, and 73 sets of solution are derived. The relation between the resulting sum Σ of weighted square deviations and q is plotted in Figure 3. A minimum value is found at $q = 2.8$. Therefore, we chose $q = 2.8$ as the initial value of q and consider it as an adjustable parameter. Then, a differential correction is performed and final solutions were obtained. The theoretical light curves are

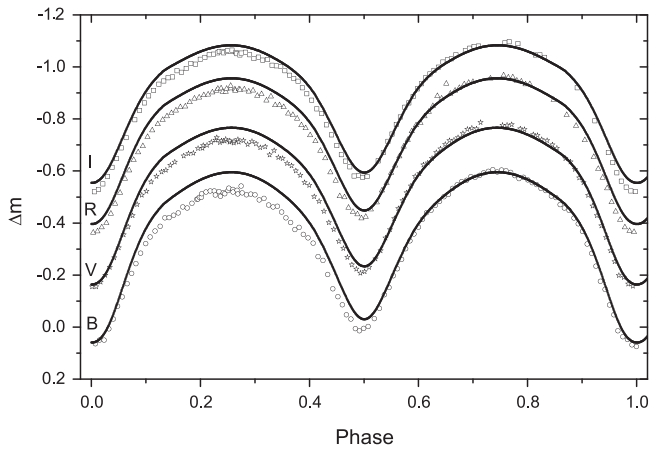


Figure 4. Theoretical light curves (solid lines) calculated without spots by using the W–D method. Open circles, stars, triangles, and squares refer to the observations in the B, V, R, and I bands, respectively.

displayed in Figure 4. As mentioned in a previous section, the observed light curves showed a negative O’Connell effect. The theoretical light curves cannot fit the data well from phase 0.08 to phase 0.55. Both components in J015100 are fast-rotating solar-type stars; they should show solar-like activity including photospheric dark spots. Therefore, the asymmetries of the light curves can be plausibly explained due to the presence of dark spots on both components. In the W–D program, each dark spot has four parameters: the latitude of spot center (θ) in degrees, the longitude of spot center (ϕ) in degrees, spot angular radius (r) in radians, and the spot temperature factor ($T_f = T_d/T_0$, where T_f is the ratio between the spot temperature T_d and the photosphere surface temperature T_0 of the star). It is shown that one dark spot on the more massive component could explain the asymmetries in the light curves, i.e., the negative O’Connell effect. The theoretical light curves that can fit the observations well are shown in Figure 5. The solutions are shown in Table 8, while the parameters of the dark spots are listed in Table 9. The corresponding geometric configurations at different phases are plotted in Figure 6.

4. DISCUSSIONS AND CONCLUSIONS

The photometric analysis in a previous section by using the W–D method suggests that J015100 is a shallow-contact binary system with a degree of contact of $f = 14.6\%$. It is a W-type system with a mass ratio of $q = M_2/M_1 = 3.128$. The less massive component is about 130 K hotter than the more massive one. These results indicate that J015100 is a contact binary below the period limit of contact binary stars. The observational properties of J015100 are similar to those of other short-period systems such as 1SWASP J074658.62+224448.5 (Jiang et al. 2015) and 2MASS 02272637+1156494 (Liu et al. 2015). The presence of these contact binary systems below in the period limit is in agreement with the conclusion obtained by Qian et al. (2015): that contact binaries below this limit are not rapidly destroyed.

By assuming that the more massive component is a K4-type main-sequence star, its mass was estimated as $M_2 = 0.70 M_\odot$ (Cox 2000). Then, the mass of the less massive and hotter component can be estimated as $M_1 = 0.22 M_\odot$ by using the derived value of q . As shown in Figure 3, the multi-color light curves are asymmetric and show a negative O’Connell effect.

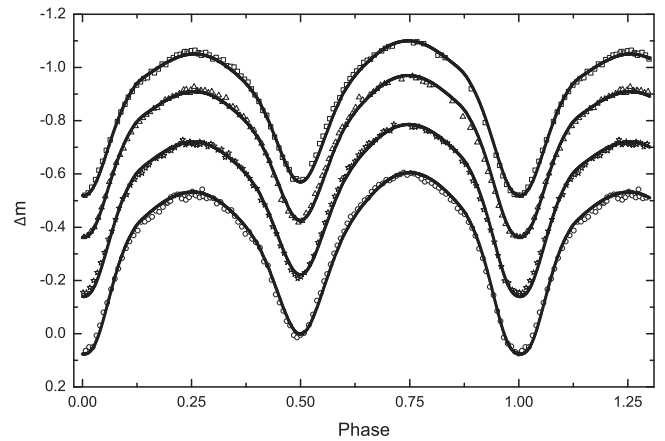


Figure 5. Theoretical light curves calculated with one dark spot on the more massive component. Symbols are the same as those in Figure 4.

Table 8
Photometric Parameters for J015100

Parameters	Photometric Elements	Errors
$q (M_2/M_1)$	3.128	± 0.011
T_2	4366 K	± 4 K
i	79.4	± 0.2
$L_1/(L_1+L_2)$ (B)	0.3172	± 0.0015
$L_1/(L_1+L_2)$ (V)	0.3080	± 0.0012
$L_1/(L_1+L_2)$ (R)	0.3045	± 0.0010
$L_1/(L_1+L_2)$ (I)	0.2997	± 0.0008
$\Omega_1 = \Omega_2$	6.6945	± 0.0166
r_1 (pole)	0.2720	± 0.0011
r_1 (side)	0.2842	± 0.0014
r_1 (back)	0.3218	± 0.0024
r_2 (pole)	0.4567	± 0.0009
r_2 (side)	0.4916	± 0.0012
r_2 (back)	0.5192	± 0.0016
The degree of contact (f)	14.6%	$\pm 2.7\%$

Table 9
Parameters of the Dark Spot on the More Massive Component

Parameters	Values
Latitude (deg)	86.52
Longitude (deg)	92.20
Radius (radian)	0.2885
$T_f(T_s/T_0)$	0.85

The asymmetries could be interpreted as the presence of a dark spot on the more massive component.

The origin and evolution of W UMa-type contact binaries were discussed by several investigators (e.g., van’t Veer 1979; Vilhu 1982; Guinan & Bradstreet 1988; Eggen & Iben 1989; Bradstreet & Guinan 1994; Qian et al. 2014b). These authors considered that this type of binary evolves into the contact configuration from initially detached binaries by AML via magnetic torques from stellar winds (Qian et al. 2013). The progenitor of J015100 may be a system similar to DV Psc, which is a K4/K5-type binary (e.g., Lu et al. 2001). It is a detached system with a very short orbital period of $0^d.30855$ (Pi et al. 2014). As discussed by Pi et al. (2014), the binary components showed strong magnetic activities, e.g., the chromospheric emission lines, the stellar spots and flare events

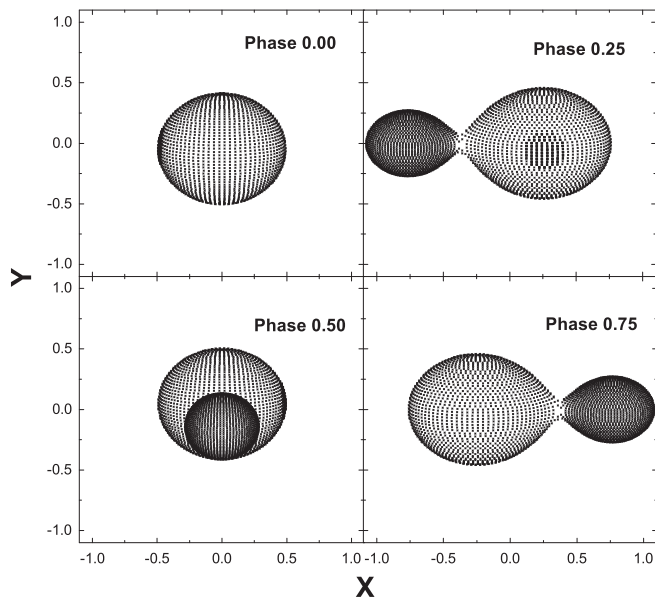


Figure 6. Geometrical structure of J015100 at phases of 0.0, 0.25, 0.5, and 0.75, respectively.

on the photospheres. The orbital shrinkage due to AML may result in the formation of a contact system similar to J015100.

This work is partly supported by Chinese Natural Science Foundation (No. 11133007 and No. 11325315), the Key Research Program of the Chinese Academy of Sciences (grant No. KGZD-EW-603), the Science Foundation of Yunnan Province (No. 2012HC011), and by the Strategic Priority Research Program “The Emergence of Cosmological Structures” of the Chinese Academy of Sciences (No.

XDB09010202). New CCD photometric observations of J015100 were obtained with the 2.4 m Thai National Telescope (TNT) of National Astronomical Research Institute of Thailand.

REFERENCES

- Becker, A. C., Bochanski, J. J., Hawley, S. L., et al. 2011, *ApJ*, **731**, 17
- Bradstreet, D. H., & Guinan, E. F. 1994, in ASP Conf. Ser., 56, *Interacting Binary Stars: A Symposium Held in Conjunction with the 105th Meeting of the ASP*, ed. A. W. Shafter (San Francisco, CA: ASP), 228
- Cox, A. N. 2000, *Allen’s Astrophysical Quantities* (4th ed.; New York: AIP)
- Davenport, J. R. A., Becker, A. C., West, A. A., et al. 2013, *ApJ*, **764**, 62
- Eggen, O. J., & Iben, I. 1989, *AJ*, **97**, 431
- Guinan, E. F., & Bradstreet, D. H. 1988, in *Formation and Evolution of Low Mass Stars*, ed. A. K. Dupree & M. T. V. T. Lago (Dordrecht: Kluwer), 345
- Jiang, L.-Q., Qian, S.-B., Zhang, J., & Zhou, X. 2015, *AJ*, **149**, 169
- Liu, L., Chen, W.-P., Qian, S.-B., et al. 2015, *AJ*, **149**, 111
- Lohr, M. E., Norton, A. J., Kolb, U. C., et al. 2012, *A&A*, **542**, A124
- Lu, W.-X., Rucinski, S. M., & Ogloza, W. 2001, *AJ*, **122**, 402
- Lucy, L. B. 1967, *ZA*, **65**, 89
- Maceroni, C., Milano, L., & Russo, G. 1982, *A&AS*, **49**, 123
- Nefs, S. V., Birkby, J. L., Snellen, I. A. G., et al. 2012, *MNRAS*, **425**, 950
- Norton, A. J., Payne, S. G., Evans, T., et al. 2011, *A&A*, **528**, A90
- Pi, Q.-F., Zhang, L.-Y., Li, Z.-M., & Zhang, X.-L. 2014, *AJ*, **147**, 50
- Pribulla, T., Rucinski, S. M., Conidis, G., et al. 2007, *AJ*, **133**, 1977
- Qian, S.-B., Jiang, L.-Q., Fernández Lajús, E., et al. 2015, *ApJL*, **798**, 42
- Qian, S. B., Jiang, L. Q., Zhu, L. Y., et al. 2014a, *CoSka*, **43**, 290
- Qian, S.-B., Liu, N.-P., Li, K., et al. 2013, *ApJS*, **209**, 13
- Qian, S.-B., Wang, J. J., Zhu, L. Y., et al. 2014b, *ApJS*, **212**, 4
- Rucinski, S. M. 1969, *AcA*, **19**, 245
- Rucinski, S. M. 1992, *AJ*, **103**, 960
- Rucinski, S. M., & Pribulla, T. 2008, *MNRAS*, **388**, 1831
- Stepień, K. 2006, *AcA*, **56**, 199
- Stepień, K. 2011, *AcA*, **61**, 139
- van Hamme, W. 1993, *AJ*, **106**, 2096
- van’t Veer, F. 1979, *A&A*, **80**, 287
- Vilhu, O. 1982, *A&A*, **109**, 17
- Wilson, R. E. 1990, *ApJ*, **356**, 613
- Wilson, R. E., & Devinney, E. J. 1971, *ApJ*, **166**, 605